Surface Chemistry

DOI: 10.1002/anie.201005002

Fully Reversible Metal Deactivation Effects in Gold/Ceria–Zirconia Catalysts: Role of the Redox State of the Support**

*José M. Cíes, Eloy del Río, Miguel López-Haro, Juan J. Delgado, Ginesa Blanco, Sebastián Collins, José J. Calvino, and Serafín Bernal**

Gold nanoparticles supported on reducible oxides are highly interesting catalytic materials. In particular, they are known to exhibit exceptional activity for CO oxidation,[1–9] low-temperature water–gas shift (LT-WGS),[10–19] and selective oxidation of CO in the presence of a large excess of hydrogen (PROX).[1,12,20–24] Despite the extraordinary research effort devoted to these catalysts, there are still some key questions about the nanostructural constitution and chemical properties of the gold sites involved in the above reactions that require further clarification.[25]

The relationship between the redox state of the support and the chemical properties of gold nanoparticles is one of these major open questions.[3,5] Its understanding, however, is critically important to fully interpret catalysis by Au/reducible oxide systems, particularly in the case of processes like LT-WGS,[15,19] PROX,[20] and hydrogenation reactions,[26] which typically occur under net reducing conditions.

To gain further information on this issue, we investigated CO adsorption on an $Au/Ce_{0.62}Zr_{0.38}O_2$ (Au/CZ) sample subjected to different redox pretreatments. In our experimental approach, FTIR spectroscopic and volumetric adsorption techniques were combined with studies on ultimate oxygen storage capacity (OSC), metal dispersion, as determined by high-resolution TEM (HRTEM) and high-angle annular dark field scanning transmission electron microscopy (HAADF-STEM), and X-ray photoelectron spectroscopy (XPS). By this approach, the influence of the redox state of the support on the CO adsorption capability of Au nanoparticles could be established on a quantitative basis. In contrast with earlier proposals suggesting that gold catalysts do not exhibit a strong metal/support interaction (SMSI) effect,[27] the results presented and discussed herein indicate that the behavior of our Au/CZ shows close resemblances with those of a number of noble metal/reducible oxide systems which are acknowledged to show this effect.[28–31]

Our experimental approach also allowed us to show that the absorption coefficient of the ν[CO(Au)] band depends on the redox state of the support. The implications of this finding for the use of integrated absorption data as a quantitative tool for characterizing the changes of CO adsorption capability occurring in gold nanoparticles supported on reducible oxides is discussed.

Figure 1 shows the ν(CO) FTIR spectra recorded on the same sample disk successively submitted to a) oxidizing treatment at 523 K (Au/CZ-O523); b) pretreatment (a) followed by reduction at 473 K (Au/CZ-O523-R473); and c) pretreatment (b) followed by reoxidation at 523 K (Au/CZ-O523-R473-O523). Further details about these pretreatments are given in the Experimental Section.

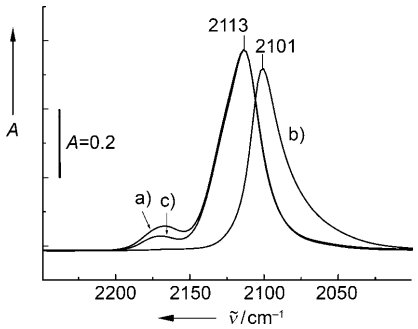

Figure 1. FTIR study of CO adsorbed on Au/CZ-O523 (a), Au/CZ-O523-R473 (b), and Au/CZ-O523-R473-O523 (c). Spectra recorded at 298 K under $P(CO) = 40$ Torr.

Comparing the spectra of Figure 1a,b reveals that the main ν(CO) band shifts from 2113 cm^{-1} for Au/CZ-O523 (Figure 1a), a position which can be assigned to CO adsorbed on Au^0 nanoparticles,[3,27,32,33] to 2101 cm^{-1} for Au/CZ-O523-R473 (Figure 1b). In accordance with a number of experimental and theoretical studies,[3,34–38] the observed redshift and the asymmetry towards the low-frequency side of the band at 2101 cm^{-1} suggest electron transfer from the reduced support to the metal nanoparticles leading to $Au^{\delta-}$ species. In addition to this band shift, the integrated absorption (IA) data (Table 1) show a second remarkable effect; the ν(CO) band intensity for Au/CZO523-R473 is approximately 15% lower

[*] J. M. Cíes, E. del Río, M. López-Haro, Dr. J. J. Delgado, Dr. G. Blanco, Dr. J. J. Calvino, Prof. S. Bernal
Departamento de Ciencia de los Materiales e Ingeniería Metalúrgica y Química Inorgánica, Facultad de Ciencias, Universidad de Cádiz
Campus Río San Pedro, 11510 Puerto Real, Cádiz (Spain)
Fax: (+34) 956-016-288
E-mail: serafin.bernal@uca.es
Dr. S. Collins
Instituto de Desarrollo Tecnológico para la Industria Química (INTEC), CONICET-UNL
Güemes 3450, S3000GLN Santa Fe (Argentina)

[**] Financial support from the Ministry of Science and Innovation of Spain/FEDER Program of the EU (Projects MAT2008-00889-NAN, and CSD2009-00013), and the Junta de Andalucía (Groups FQM-110 and FQM-334) is acknowledged. The ceria-zirconia sample was kindly donated by Grace Davison Company. E.R.S. acknowledges the Ministry of Education of Spain for a predoctoral grant. J.M.C. and M.L.H. are grateful to the Ministry of Science and Innovation of Spain for predoctoral grants.

Supporting information for this article is available on the WWW under http://dx.doi.org/10.1002/anie.201005002.

Table 1: Metal dispersion (D and D_{4-7}), ν(CO) IR band integrated absorption, and volumetric CO adsorption data for Au/CZ catalyst and the corresponding support (CZ) pretreated as indicated.

Sample	Metal dispersion[a] (D=Au_S/Au_T)	Contribution to D of Au_S with CN ≤ 7[a] (D_{4-7}=Au_S(CN≤7)/Au_T)	IA for ν(CO) band[b]	Amount of CO adsorbed on Au and CZ[c]	Amount of CO adsorbed on Au[d]	IA/Q_{CO} ratio[e]
Au/CZ-O523	0.47	0.26	20.2	22.0	19.4	1.0
Au/CZ-O523-R473	0.48	0.27	17.1	12.0	10.9	1.6
Au/CZ-O523-R473-O523	0.48	0.26	19.7	21.9	19.3	1.0
CZ-O523	–	–	0.7	2.6	–	0.3
CZ-O523-R773	–	–	0.3	1.1	–	0.3

[a] D and D_{4-7} determined by application to the experimental Au nanoparticle size distributions of the methodology described in Ref. [40] (for more details see Table SI.1 in the Supporting information). [b] As determined by integration of the ν(CO) FTIR band recorded at 298 K under P_{CO} = 40 Torr for the three Au/CZ samples (Figure 1) and the bare support pretreated as indicated. [c] Amount of CO (μmol g^{-1}_{sample}) adsorbed on Au/CZ and CZ samples as determined from the second of the two consecutive volumetric isotherms recorded at 308 K. Data corresponding to P_{CO} = 40 Torr. [d] Amount of CO (μmol g^{-1}_{sample}) adsorbed on the supported Au nanoparticles as determined from the difference of the second isotherm data at P_{CO} = 40 Torr for Au/CZ and CZ support showing a similar redox state. [e] Integrated absorption/amount of CO (Q_{CO}) adsorbed on either Au nanoparticles (6th column) or the support (bottom part of 5th column).

than that for Au/CZ-O523. Interestingly, these two effects can be fully reversed by reoxidation of Au/CZ-O523-R473 at 523 K (Figure 1c). As shown in Figure 1, the ν(CO) spectra for Au/CZ-O523 and Au/CZ-O523-R473-O523 samples are almost superimposable, and their corresponding integrated absorptions (Table 1) are accordingly very similar.

The results above strongly suggest the occurrence of a perfectly reversible SMSI effect, like that earlier reported for other noble metals highly dispersed on different reducible supports.[28–31] If so, the change in the chemical properties of the Au nanoparticles could be determined by the redox state of the support. To confirm this proposal, a number of additional studies were performed.

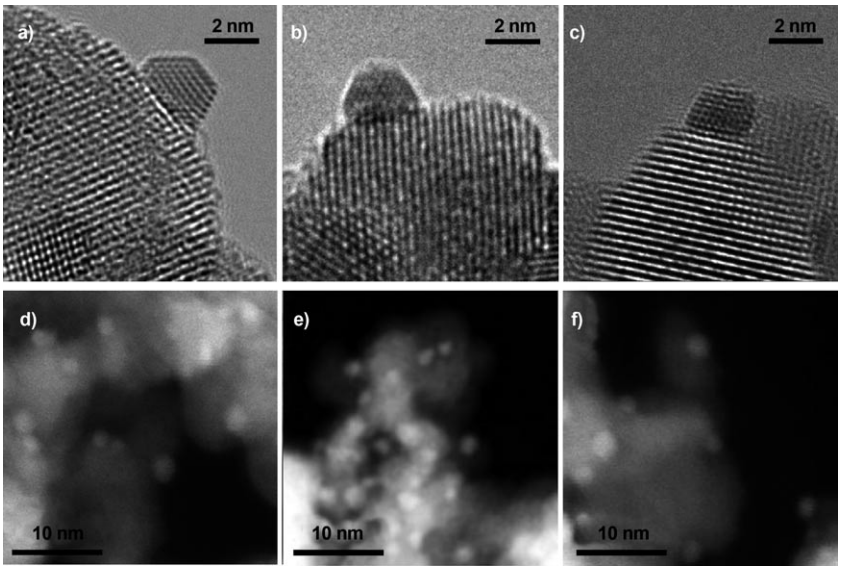

Figure 2. Representative HREM (a–c) and HAADF-STEM (d–f) images of Au/CZ-O523 (a and d), Au/CZ-O523-R473 (b and e), and Au/CZ-O523-R473-O523 (c and f) samples.

We have first checked the influence of the different thermochemical pretreatments on gold dispersion by HREM and HAADF-STEM, which were recently shown to provide rather detailed nanostructural information about gold supported on oxides of heavy elements, such as ceria–zirconia.[39,40] Figure 2 shows some representative images for the three investigated Au/CZ catalysts. Their analysis gave the gold nanoparticle size distributions reported in Figure SI.1 (Supporting Information).

As we showed in reference [40], the combination of computer nanostructural modeling with experimental gold nanoparticle size distribution offers a way for determining not only the overall metal dispersion ($D = Au_S/Au_T$, where Au_S is the number of surface gold atoms, and Au_T the total number of gold atoms) associated to a certain size distribution, but also the contribution to D of the gold surface atoms showing a specific coordination number (CN = j), D_j = (Au_S with CN = j)/Au_T. In agreement with reference [40], j values ranging from 4 to 9 were observed in this work. The contribution to D of surface atoms with CN ≤ j may easily be determined as $D_{4-j} = \sum_{4-j} D_j$. By following this approach, it was shown in reference [40] that for adsorption experiments at 308 K under P(CO) ranging from 0 to 300 Torr, the only Au surface atoms involved in the process are those with $j \leq 7$, that is, the saturation coverage could be measured by D_{4-7}.

By applying this methodology to the nanoparticle size distributions determined for our Au/CZ samples (Figure SI.1 in the Supporting Information) the set of D_j and D_{4-j} data reported in Table SI.1 (Supporting Information) were obtained. Those specifically corresponding to D and D_{4-7} are also included in Table 1. As deduced from these values, the pretreatments successively applied to our catalyst do not significantly modify either D nor D_{4-7} to within the experimental error in our estimate of the dispersion values suggested by the analysis (±2%; Figure SI.2 in the Supporting Information). Accordingly, we can conclude that the reversible change of intensity in the ν(CO) spectra reported in Figure 1 cannot be interpreted in terms of parallel modifications of the metal dispersion.

Evaluating the influence of the redox state of the support on the absorption coefficient of the ν[CO(Au)] band is also a relevant issue. Otherwise, the meaning of the change of integrated absorption data reported in Table 1 would be uncertain. Gaining quantitative information about the CO specifically chemisorbed on gold is therefore critically important. For this purpose, we applied a volumetric adsorption routine proposed earlier.[40,41] This approach is based on an earlier FTIR spectroscopic study,[42] according to which, under CO pressure at room temperature, three major components contribute to the overall FTIR spectrum of CO adsorbed on Au/CZ catalysts: 1) Carbonate species strongly chemisorbed on the support, for which bands are observed in the range 1000–1700 cm^{-1}; they remain almost unaffected by 30 min evacuation at 308 K.[42] 2) CO adsorbed on Au, characterized by bands in the range 2000–2200 cm^{-1}, which are almost completely removed by 30 min evacuation at 308 K.[42] 3) CO weakly adsorbed on cationic sites at the surface of the support may also be observed.[42] The associated bands, which typically occur in the 2140–2200 cm^{-1} region, are easily eliminated by 30 min evacuation at room temperature.[42] Therefore, the second of a series of two consecutive isotherms at 308 K, separated by 30 min evacuation at the same temperature, would measure the last two contributions to the overall adsorption of CO on Au/CZ.[41] Application of this routine to the bare CZ support would allow us to determine the amount of CO weakly adsorbed on its surface cations. Hence, the difference between the second isotherms for Au/CZ and CZ would actually measure the amount of CO specifically adsorbed on the gold nanoparticles. Table SI.2 (Supporting Information) reports the quantitative data corresponding to the second isotherms at 308 K for the Au/CZ and CZ samples subjected to the different pretreatments applied in this work.

The eventual influence on the adsorptive behavior of the redox state of the CZ support was also taken into account. For this purpose, CO adsorption isotherms were recorded on CZ-O523 and CZ-O523-R773 samples; that is, the oxide pretreated like the Au/CZ-O523 catalyst, and that reduced at 773 K by following a routine similar to that applied to Au/CZ-O523-R473, CZ-O523-R773. The choice of a reduction temperature of 773 K was based on a thermogravimetric study of ultimate oxygen storage capacity (OSC)[43–45] carried out under similar reduction conditions to those applied in reference [45], that is, 1 h treatment under flowing 5 % H_2/Ar at each of the selected temperatures. The corresponding data are reported in Table SI.3 (Supporting Information). According to this study, the ultimate OSC values for Au/CZ-O523-R473 and CZ-O523-R773 are rather similar: 26 and 29 %, respectively. Therefore, the pure CZ reduced at 773 K was used as a reference for describing weak CO adsorption on the support cations of Au/CZ-O523-R473.

Table 1 summarizes the quantitative data resulting from the above volumetric adsorption study. The fifth column reports the total amount of CO weakly adsorbed on Au/CZ and CZ samples pretreated as indicated. The amounts of CO specifically adsorbed on Au, reported in the sixth column of Table 1, were determined by difference of the data reported in the fifth column for Au/CZ and the CZ support showing a similar redox state; that is, the fully oxidized support (CZ-O523) for Au/CZ-O523 and Au/CZ-O523-R473-O523 catalysts, and the similarly reduced one (CZ-O523-R773) for Au/CZ-O523-R473. The resulting data—19.4 μmol g^{-1} and 19.3 μmol g^{-1} for Au/CZ-O523 and Au/CZ-O523-R473-O523, respectively, and 10.9 μmol g^{-1} for Au/CZ-O523-R473—fully confirm the occurrence of a reversible change in the CO adsorption capacity of the gold nanoparticles. Our observation is consistent with some earlier studies, according to which gold nanoparticles supported on a reduced ceria thin film show a lower CO adsorption energy than those supported on an oxidized one.[46]

Comparison of data reported in columns 5 and 6 of Table 1 clearly indicates that the loss of adsorption capacity of 44 % deduced from the volumetric study is significantly larger than that of 15 % suggested by the integrated absorption data for the ν[CO(Au)] band. Accordingly, we may conclude that the absorption coefficient for this band is sensitive to the redox state of the support. To evaluate this effect, we determined the ratio between the integrated absorption and the amount of CO adsorbed on gold, $IA/Q_{CO(Au)}$, for the three catalysts. As deduced from the seventh column of Table 1, the $IA/Q_{CO(Au)}$ values are found to be 1.0 for Au/CZ-O523 and Au/CZ-O523-R473-O523 and significantly larger (1.6) for Au/CZ-O523-R473.

The reversible changes of CO adsorption capacity and ν[CO(Au)] band absorption coefficient reported above are likely to be determined by parallel modifications in the electronic properties of the Au nanoparticles. Accordingly, we performed an XPS study of the Au/CZ sample successively subjected to the three pretreatments. The corresponding Au 4f XP spectra are reported in Figure SI.3 (Supporting Information). The binding energy (BE) for the Au $4f_{7/2}$ component was found to be 84.5 eV for Au/CZ-O523 and Au/CZ-O523-R473-O523, and 84.3 eV for Au/CZ-O523-R473, that is, a reversible shift in the BE occurs for this gold signal. As discussed in references [46,47], both initial and final state could in principle play a role in determining the BE in gold supported on ceria thin films. Factors like Au oxidation state, charge transfer, and the coordination number of gold atoms, that is, the metal nanoparticle size, could influence the initial state, whereas the effects on the final state are mainly related to the screening and delocalization of the holes created by the photoionization process. These latter effects are known to depend on the nature and particle size of the supported metal phase.[47] In the present case, the similarity of the Au nanoparticle size distributions and dispersion data reported in Figure SI.1 (Supporting Information) and Table 1, respectively, allows us to reasonably exclude size-dependent effects as a relevant cause of the observed BE shift. Therefore, initial-state effects associated with charge transfer from the reduced support to the metal seem to be the most likely origin of the shift to lower BE observed for Au/CZ-O523-R473.

In conclusion, application of our original approach combining FTIR, measurements of volumetric adsorption and ultimate OSC with HRTEM, HAADF-STEM, and XPS studies allowed us to show the occurrence of a fully reversible change in the chemisorptive properties of gold nanoparticles

supported on a $Ce_{0.62}Zr_{0.38}O_2$ mixed oxide. This effect, which could be quantitatively assessed, is induced by alternating oxidizing and reducing pretreatments at quite moderate temperatures. All of the reported results are fully consistent with the occurrence of an SMSI-like effect, mainly determined by the modifications induced in the electronic properties of the Au nanoparticles by the successive changes in the redox state of the support. No evidence of metal decoration, an effect often reported for catalysts in the SMSI state, could be deduced from our study. This observation, however, is fully consistent with earlier investigations on M/CZ catalysts (M = Rh, Pd, or Pt), in which this effect was absent even in samples reduced at much higher temperature.[31]

In contrast with most of the studies presently available, which dealt with model systems prepared and characterized under rather unconventional conditions,[3,35–37,46,47] the results reported herein were obtained on a powder catalyst prepared by a common deposition/precipitation procedure. Both the oxidizing and reducing pretreatments applied in our work are very close to those commonly used in the activation of powdered gold catalysts. Therefore, our findings may be fruitfully used in the analysis of many other results from the literature dealing with ceria-based gold catalysts. Moreover, the applied reduction temperature of 473 K is within the range in which some very relevant reactions like LT-WGS, PROX, and numerous hydrogenation processes, which typically occur under net reducing conditions, are carried out.[15,19,20,24] This is a remarkable observation, because, under the experimental conditions of these reactions, strong modifications of the chemical properties of the gold nanoparticles, and therefore, of their catalytic behavior may be induced by the reduced support.

Finally, we have shown that the absorption coefficient for the ν[CO(Au)] IR band of Au/CZ is sensitive to the redox state of the support. This finding precludes straightforward use of integrated IR absorption data in quantitative evaluations of the metal deactivation/regeneration effects associated with alternating redox pretreatments.

Experimental Section

The 2.6 wt% $Au/Ce_{0.62}Zr_{0.38}O_2$ (Au/CZ) catalyst, with a BET surface area of 63 $m^2 g^{-1}$, was prepared by a homogeneous deposition/precipitation procedure similar to that followed in ref. [48] Details of the preparation routine are reported elsewhere.[42] According to the XRD, nanostructural, and nanoanalytical studies carried out on the CZ support, it consists of a homogeneous single-phase sample.

FTIR spectra for CO adsorbed on both Au/CZ and CZ samples were recorded at 298 K at $P(CO) = 40$ Torr (1 Torr = 133 Pa) on a Bruker Vertex 70 instrument equipped with a deuterated triglycine sulfate (DTGS) detector. Typically, 100 scans at a resolution of 4 cm^{-1} were averaged. A self-supported disk of the powder sample was placed in a quartz cell with CaF_2 windows, attached to a metallic high-vacuum manifold equipped with a turbo molecular pump (residual pressure $< 10^{-6}$ Torr). The whole study was carried out on a single disk successively subjected to the following in situ pretreatments: a) heating in a flow of 5% O_2/He at 523 K (1 h), followed by 1 h evacuation at 523 K; the resulting sample is referred to as Au/CZ-O523; b) oxidizing treatment a) followed by reduction at 473 K (1 h) in flow of 5% H_2/Ar and further evacuation at 473 K (1 h) to give sample Au/CZ-O523-R473; and c) reoxidation of Au/CZ-O523-R473 by routine a), giving sample Au/CZ-O523-R473-O523.

Catalysts pretreated as in the FTIR study were also investigated by HRTEM and HAADF-STEM. HRTEM images were recorded on a JEOL2010-F microscope with 0.19 nm spatial resolution under Scherzer defocus conditions. HAADF-STEM images were obtained by using an electron probe of 0.5 nm of diameter at a diffraction camera length of 10 cm.

Volumetric adsorption experiments were performed on a Micromeritics ASAP-2020 instrument. The CO isotherms were all recorded at 308 K. The amount of Au/CZ catalyst was 200 mg. The studies consisted of two consecutive isotherms of $P(CO)$ range 0–40 Torr with 30 min evacuation at 308 K inbetween. They were carried out on a single catalyst sample successively pretreated as in the FTIR study. Double CO adsorption isotherms were also recorded for the CZ support, either submitted to the so-called O523 pretreatment (CZ-O523) or to the oxidizing pretreatment mentioned above followed by 1 h reduction under flowing 5% H_2/Ar at 773 K and 1 h evacuation at 773 K (CZ-O523-R773).

To characterize the redox state of CZ in both the CZ support and the Au/CZ catalyst, ultimate oxygen storage capacity (OSC) measurements as defined in refs. [43–45] were performed by thermogravimetric (TG) analysis.[45] Samples were first subjected to oxidizing pretreatment at 523 K, and then they were heated under flowing 5% H_2/Ar in a stepwise manner at temperatures ranging from 473 to 973 K. Duration of the isothermal steps: 1 h. Parallel OSC data, as determined by O_2 volumetric adsorption at 523 K on samples pre-reduced in the same way were in good agreement with those determined from the TG study. This shows that the oxidizing treatment at 523 K ensures full reoxidation of the pre-reduced samples.

A self-supported wafer of Au/CZ successively subjected to the series of pretreatments described above was also investigated by XPS on a Kratos Axis Ultra DLD instrument equipped with a catalytic cell allowing a clean transfer of the pretreated samples to the analytical chamber. Spectra were recorded with monochromatized $Al_{K\alpha}$ radiation (1486.6 eV) with a selected X-ray power of 150 W. The spectrometer was operated in the fixed analyzer transmission (FAT) mode with a pass energy of 20 eV. Surface charging effects were compensated by using the Kratos coaxial neutralization system. The binding energy (BE) scale was calibrated with respect to the Zr $3d_{5/2}$ component in the mixed-oxide support and fixed to 182.64 eV. Spectral processing was performed with CasaXPS software. Deconvolution studies on the Au 4f core level were carried out by using Doniach–Sunjic-type line shapes and Shirley-type backgrounds.

Received: August 10, 2010
Published online: ■■ ■■, 2010

Keywords: carbon monoxide · ceria–zirconia · chemisorption · gold · supported catalysts

[1] S. Carrettin, P. Concepción, A. Corma, J. M. López-Nieto, V. F. Puntes, *Angew. Chem.* **2004**, *116*, 2592 – 2594; *Angew. Chem. Int. Ed.* **2004**, *43*, 2538 – 2540.
[2] A. M. Venezia, G. Pantaleo, A. Longo, G. Di Carlo, M. P. Casaletto, F. L. Liotta, G. Deganello, *J. Phys. Chem. B* **2005**, *109*, 2821 – 2827.
[3] M. Chen, D. W. Goodman, *Acc. Chem. Res.* **2006**, *39*, 739 – 746.
[4] F. Moreau, G. C. Bond, *Catal. Today* **2006**, *114*, 362 – 368.
[5] Y. Denkwitz, Z. Zhao, U. Hormann, U. Kaiser, V. Plzak, R. J. Behm, *J. Catal.* **2007**, *251*, 437 – 442.
[6] A. A. Herzing, C. J. Kiely, A. F. Carley, P Landon, G. J. Hutchings, *Science* **2008**, *321*, 1331 – 1335.
[7] Z. Zhou, S. Kooi, M. Flytzani-Stephanopoulos, H. Saltsburg, *Adv. Funct. Mater.* **2008**, *18*, 2801 – 2807.

[8] X. S. Huang, H. Sun, L. C. Wang, Y. M. Liu, K. N. Fan, Y. Cao, *Appl. Catal. B* **2009**, *90*, 224 – 232.
[9] A. Tost, D. Widmann, R. J. Behm, *J. Catal.* **2009**, *266*, 299 – 307.
[10] R. Burch, *Phys. Chem. Chem. Phys.* **2006**, *8*, 5483 – 5500.
[11] R. Leppelt, B. Schumacher, V. Plzak, M. Kinne, R. J. Behm, *J. Catal.* **2006**, *244*, 137 – 152.
[12] W. Deng, M. Flytzani-Stephanopoulos, *Angew. Chem.* **2006**, *118*, 2343 – 2347; *Angew. Chem. Int. Ed.* **2006**, *45*, 2285 – 2289.
[13] Y. Denkwitz, A. Karpenko, V. Plzak, R. Leppelt, B. Schumacher, R. J. Behm, *J. Catal.* **2007**, *246*, 74 – 90.
[14] A. Karpenko, Y. Denkwitz, V. Plzak, J. Cai, R. Leppelt, B. Schumacher, R. J. Behm, *Catal. Lett.* **2007**, *116*, 105 – 115.
[15] A. Goguet, R. Burch, Y. Chen, C. Hardacre, P. Hu, R. W. Joyner, F. Meunier, B. S. Mun, D. Thompsett, D. Tibiletti, *J. Phys. Chem. C* **2007**, *111*, 16927 – 16933.
[16] W. Deng, A. I. Frenkel, S. Rui, M. Flytzani-Stephanopoulos, *J. Phys. Chem. C* **2008**, *112*, 12834 – 12840.
[17] A. Abd El-Moemen, A. Karpenko, Y. Denkwitz, R. J. Behm, *J. Power Sources* **2009**, *190*, 64 – 75.
[18] J. B. Park, J. Graciani, J. Evans, D. Stacchiola, S. Ma, P. Liu, A. Nambu, J. Fernández Sanz, J. Hrebk, J. A. Rodríguez, *Proc. Natl. Acad. Sci. USA* **2009**, *106*, 4975 – 4980.
[19] H. Daly, A. Goguet, C. Hardacre, F. C. Meunier, R. Pilasombat, D. Thompsett, *J. Catal.* **2010**, *273*, 257 – 265.
[20] D. L. Trimm, *Appl. Catal. A* **2005**, *296*, 1 – 11.
[21] F. Arena, P. Famulari, G. Trunfio, G. Bonura, F. Frusteri, L. Spadaro, *Appl. Catal. B* **2006**, *66*, 81 – 91.
[22] M. Azar, V. Caps, F. Morfin, J. L. Rousset, A. Piednoir, J. C. Bertolini, L. Piccolo, *J. Catal.* **2006**, *239*, 307 – 312.
[23] L. H. Chang, N. Sasirekha, Y. W. Chen, *Catal. Commun.* **2007**, *8*, 1702 – 1710.
[24] G. Avgouropoulos, M. Manzoli, F. Boccuzzi, T. Tabakova, J. Papavasiliou, T. Ioannides, V. Idakiev, *J. Catal.* **2008**, *256*, 237 – 247.
[25] A. Chiorino, M. Manzoli, F. Menegazzo, M. Signoretto, F. Vindigni, F. Pinna, F. Boccuzzi, *J. Catal.* **2009**, *262*, 169 – 176.
[26] F. Cardenas-Lizana, S. Gómez-Quero, N. Perret, M. A. Keane, *Gold Bull.* **2009**, *42*, 124 – 132.
[27] R. Meyer, C. Lemire, Sh. K. Shaikhutdinov, H.-J. Freund, *Gold Bull.* **2004**, *37*, 72 – 124.
[28] S. J. Tauster, S. C. Fung, J. Garten, *J. Am. Chem. Soc.* **1978**, *100*, 170 – 175.
[29] J. Sanz, J. P. Belzunegui, J. M. Rojo, *J. Am. Chem. Soc.* **1992**, *114*, 6749 – 6754.
[30] S. Bernal, J. J. Calvino, M. A. Cauqui, J. M. Gatica, C. Larese, J. A. Pérez-Omil, J. M. Pintado, *Catal. Today* **1999**, *50*, 175 – 206.
[31] J. M. Gatica, R. T. Baker, P. Fornasiero, S. Bernal, J. Kaspar, *J. Phys. Chem. B* **2001**, *105*, 1191 – 1199.
[32] T. Risse, S. Shaikhutdinov, N. Nilius, M. Sterrer, H. J. Freund, *Acc. Chem. Res.* **2008**, *41*, 949 – 956.
[33] F. Vindigni, M. Manzoli, A. Chiorino, F. Boccuzzi, *Gold Bull.* **2009**, *42*, 106 – 112.
[34] B. Yoon, H. Häkkinen, U. Landman, A. S. Wörz, J. M. Antonietti, S. Abbet, K. Judai, U. Heiz, *Science* **2005**, *307*, 403 – 407.
[35] M. Sterrer, M. Yulikov, E. Fischbach, M. Heyde, H. P. Rust, G. Pacchioni, T. Risse, H. J. Freund, *Angew. Chem.* **2006**, *118*, 2692 – 2695; *Angew. Chem. Int. Ed.* **2006**, *45*, 2630 – 2632.
[36] A. S. Wörz, U. Heiz, F. Cinquini, G. Pacchioni, *J. Phys. Chem. B* **2005**, *109*, 18418 – 18426.
[37] A. Fielicke, G. von Helden, G. Meijer, B. Simard, D. M. Rayner, *J. Phys. Chem. B* **2005**, *109*, 23935 – 23940.
[38] M. Manzoli, F. Bocuzzi, A. Chiorino, F. Vindigni, W. Deng, M. Flytzani-Stephanopoulos, *J. Catal.* **2007**, *245*, 308 – 315.
[39] J. C. González, J. C. Hernández, M. López-Haro, E. del Río, J. J. Delgado, A. B. Hungría, S. Trasobares, S. Bernal, P. A. Midgley, J. J. Calvino, *Angew. Chem.* **2009**, *121*, 5417 – 5419; *Angew. Chem. Int. Ed.* **2009**, *48*, 5313 – 5315.
[40] M. López-Haro, J. J. Delgado, J. M. Cíes, E. del Río, S. Bernal, R. Burch, M. A. Cauqui, S. Trasobares, J. A. Pérez-Omil, P. Bayle-Guillemaud, J. J. Calvino, *Angew. Chem.* **2010**, *122*, 2025 – 2029; *Angew. Chem. Int. Ed.* **2010**, *49*, 1981 – 1985.
[41] J. M. Cíes, J. J. Delgado, M. López-Haro, R. Pilasombat, J. A. Pérez-Omil, S. Trasobares, S. Bernal, J. J. Calvino, *Chem. Eur. J.* **2010**, *16*, 9536 – 9543.
[42] S. E. Collins, J. M. Cíes, E. del Río, M. López-Haro, S. Trasobares, J. J. Calvino, J. M. Pintado, S. Bernal, *J. Phys Chem. C* **2007**, *111*, 14371 – 14379.
[43] D. Duprez, C. Descorme in *Catalysis by Ceria and Related Materials* (Ed.: A. Trovarelli), Imperial College, London, **2002**, chap. 7, pp. 243 – 280.
[44] M. P. Yeste, J. C. Hernández, S. Bernal, G. Blanco, J. J. Calvino, J. A. Pérez-Omil, J. M. Pintado, *Chem. Mater.* **2006**, *18*, 2750 – 2757.
[45] M. P. Yeste, J. C. Hernández, S. Bernal, G. Blanco, J. J. Calvino, J. A. Pérez-Omil, J. M. Pintado, *Catal. Today* **2009**, *141*, 409 – 414.
[46] C. J. Weststrate, R. Westerström, E. Lundgren, A. Mikkelsen, J. N. Andersen, A. Resta, *J. Phys. Chem. C* **2009**, *113*, 724 – 728.
[47] M. Baron, O. Bondarchuk, D. Stacchiola, S. Shaikhutdinov, H. J. Freund, *J. Phys. Chem. C* **2009**, *113*, 6042 – 6049.
[48] R. Zanella, S. Giorgio, C. R. Henry, C. Louis, *J. Phys. Chem. B* **2002**, *106*, 7634 – 7642.

Communications

Surface Chemistry

J. M. Cíes, E. del Río, M. López-Haro, J. J. Delgado, G. Blanco, S. Collins, J. J. Calvino, S. Bernal* ____ ▮▮▮▮–▮▮▮▮

Fully Reversible Metal Deactivation Effects in Gold/Ceria–Zirconia Catalysts: Role of the Redox State of the Support

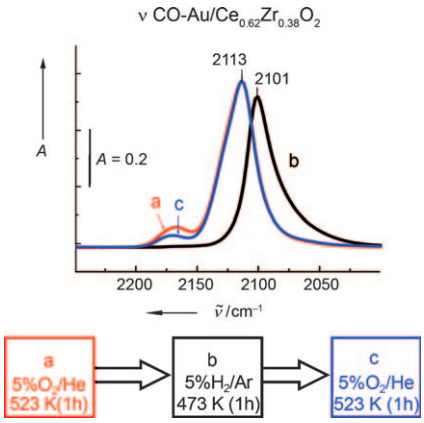

Strong and reversible modification of the chemical properties of supported Au nanoparticles caused by alternating oxidizing (a and c) and reducing (b) pretreatment of $Au/CeO_2–ZrO_2$ catalysts were revealed by a methodology that combines FTIR spectroscopy (see picture), studies on the volumetric adsorption of CO and ultimate oxygen storage capacity, determination of metal dispersion by electron microscopy, and X-ray photoelectron spectroscopy.